

pubs.acs.org/journal/estlcu Letter

Atmospheric Progression of Microcystin-LR from Cyanobacterial Aerosols

Myoseon Jang,* David E. Berthold, Zechen Yu, Cecilia Silva-Sanchez, H. Dail Laughinghouse IV, Nancy D. Denslow, and Sanghee Han



Cite This: https://dx.doi.org/10.1021/acs.estlett.0c00464



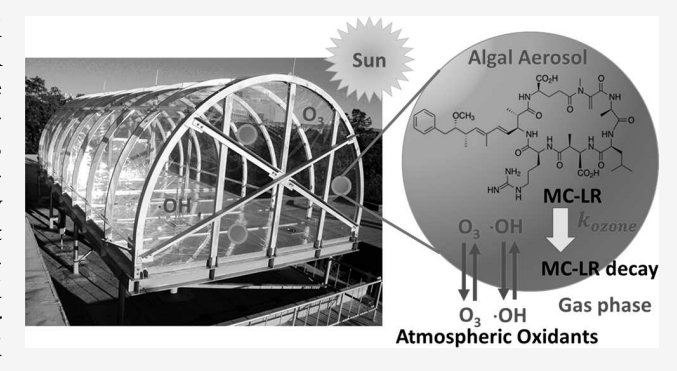
ACCESS

Metrics & More

Article Recommendations

Supporting Information

ABSTRACT: The potential for exposure to aerosolized algal toxins during harmful algal blooms has not been well studied. A fundamental question about the longevity of algal toxins in the aerosol phase remains. In this study, the influence of environmental factors such as sunlight and atmospheric oxidants (e.g., ozone and OH radicals) on the lifetime of microcystin-LR (MC-LR), which is known to be the most toxic of the MCs produced by cyanobacteria, was investigated. A cyanobacterial culture aliquot (Microcystis aeruginosa and Dolichospermum sp.) spiked with MC-LR was nebulized into a large outdoor photochemical chamber and atmospherically aged in the presence and absence of sunlight or ozone. The concentrations of MC-LR in aerosol were measured using liquid chromatography/tandem mass spectrometry and the



enzyme-linked immunosorbent assay (ELISA) for atmospheric aging of aerosols. With 61.5 nm 3 m $^{-3}$ gaseous ozone, the second-order rate constant of ELISA-based MC-LR in *M. aeruginosa* aerosol was approximately (3.91 \pm 0.17) \times 10 5 M $^{-1}$ s $^{-1}$ (54 min lifetime). Because of the involvement of OH radicals, the daytime degradation of MC-LR was significantly faster than that at night with the same amount of ozone in the chamber air. We conclude that under natural sunlight, MC-LR in cyanobacterial aerosols quickly decays through heterogeneous chemistry with atmospheric oxidants but can still impact neighboring communities.

■ INTRODUCTION

Over the past half-century, freshwater harmful algal bloom research has revealed a wide range of toxins produced by cyanobacteria.1 These toxins represent a range of threats to ecosystem, animal, and human health.²⁻⁶ There is a growing consensus that anticipated future changes in climate will exacerbate the threats associated with toxic cyanobacteria by increasing the frequency and intensity of blooms. 5,7,8 While the risk of exposure via direct ingestion of effected waters has attracted considerable attention,⁹ the potential for exposure to aerosolized toxins is less understood, ¹⁰ despite clear concerns about the health risks for persons living, working, or recreating near freshwater bodies subject to intense cyanobacterial blooms. 11 Recent research has shown the presence of the toxin microcystin (MC) in air samples collected around lakes experiencing blooms of the cyanobacterium *Microcystis* aeruginosa (Kützing). 10,12-14 However, questions about the longevity of toxins in the aerosol phase remain, including the effects of various environmental factors such as sunlight and the presence of key atmospheric oxidants such as ozone, OH radicals, and nitrate radicals.

Microcystins are cyclic heptapeptides that include a unique β -amino acid (ADDA) (Figure S1). The ADDA unit has been shown to play acute roles in the mode of action of MC binding

and inhibiting protein phosphatases in mammalian cells. Remarkably, the production of polyclonal antibodies against MC congeners is not very different because of the relative immunodominance of ADDA in various MCs. 16,17 Similar to the reaction of alkenes in the atmosphere, 18,19 the conjugated alkene in ADDA reacts with atmospheric oxidants. Thus, the toxicity due to ADDA can decrease via heterogeneous oxidation in aerosols. Cyanobacterial aerosols from water spray also contain various other substances besides toxins (i.e., MCs), such as chlorophylls. Porphyrin moieties in chlorophylls are photosensitizers and are easily excited using visible wavelength radiation (600–650 nm), and the singlet-excited porphyrins rapidly transform into triplet-excited states, which are longer-lived and can transfer their energy to triplet oxygen to form singlet oxigen. The singlet oxygen can either be irradiated by overtone vibration modes of water molecules and hydrocarbons 23,24 or produce other reactive

Received: June 11, 2020 Revised: August 10, 2020 Accepted: August 11, 2020 Published: August 11, 2020



Table 1. Chamber Experimental Conditions for Investigating the Atmospheric Process of MC-LR in Cyanobacterial Aerosols in the UF-APHOR Chamber

experiment	date (month/ day/year)	aerosol	$\begin{array}{c} \text{sunlight} \\ \left(W/m^2\right) \end{array}$	T (K)	RH (%)	$[aerosol]^c \ (\mu g/m^3)$	injected MC-LR d (ng/m 3)	$ \begin{array}{c} ozone \\ (nm^3 \ m^{-3}) \end{array} $	comments
A	5/5/2020	M. aeruginosa ^b	night	291-293	70-74	96.1	451	61.5	LC-MS/MS, ELISA
В	1/22/2020	Anabaena sp. ^a	3.9-19.9	276-296	20-59	5.1	123	3-27	LC-MS/MS
С	2/21/2020	Anabaena sp. ^a	0-8.0	278-288	74-100	15.1	186	3-15	LC-MS/MS, ELISA
D	2/21/2020	silica	0-8.5	281-288	79–96	32.1	142	3-17	LC-MS/MS, ELISA
E	5/5/2020	M. aeruginosa ^b	0-18.0	291-306	44-86	90.0	422	2-17	LC-MS/MS, ELISA

"Commercially available Anabaena (=Dolichospermum). The MC-LR measured in cyanobacterial aerosol originates mostly from the spiked MC-LR. LC-MS/MS data showed that the concentrations of authentic MCs (extracellular and intracellular combined) in Anabaena sp. were negligible. ^bM. aeruginosa BLCC-F108 is a high-MC-producing strain that was isolated from Lake Okeechobee, Florida, during a massive algal bloom in 2019 and cultured at UF/IFAS. LC-MS/MS data showed that the concentrations of the authentic MCs (extracellular and intracellular combined) in M. aeruginosa were negligible. ^cThe concentration of cyanobacterial aerosol in the chamber air is calculated using SMPS data (algal aerosol + water) assuming that the density of aerosol is 1 g/mL. The water fraction of total aerosol was ~22% at 70% RH. The error associated with SMPS data is 3%. ^dThe concentration of the MC-LR that was injected into the chamber is calculated using SMPS data and the mass ratio of MC-LR to dried algae (50:8320 for experiments A and E, 50:2000 for experiment B, 50:3750 for experiment C, and 50:6000 for experiment D). To measure the dry cyanobacterial mass, 100 μL algae aliquots were spiked on the preweighed filter, dried using the tank air, and weighed using the analytical balance at 25% RH. The dry cyanobacterial mass concentrations of experiments A–C were 3.3, 0.8, and 0.75 mg/mL, respectively. The detailed information for the calculation of the concentration of LC-MR in chamber air can be found in the Supporting Information.

oxygen species (ROS) that can induce oxidation of various molecules, including MCs in cyanobacterial aerosols.

This study focuses on the atmospheric process of MC-LR (a ubiquitous, abundant, and toxic microcystin) in aerosolized cyanobacteria. The experiments employed a state-of-the-art technology developed at the University of Florida (UF), centered on the Atmospheric Photochemical Outdoor Reactor (UF-APHOR) dual chambers, ²⁵⁻²⁷ which allow for the quantification of atmospheric aging of cyanobacterial toxins, under a range of atmospheric conditions such as sunlight, temperature (*T*), relative humidity (RH), ozone, and OH radicals (Figure S2). The degradation of MC-LR was monitored using liquid chromatography/tandem mass spectrometry (LC-MS/MS) and the enzyme-linked immunosorbent assay (ELISA) over the course of the chamber experiment.

■ MATERIALS AND METHODS

Chamber Operation. The chamber experiment began with a commercially available Anabaena (=Dolichospermum) strain (VWR International LLC), and experiments were extended to include M. aeruginosa BLCC-F108 (BLCC, FLREC, UF/IFAS). Both cyanobacterial strains chosen (Dolichospermum and Microcystis) are common freshwater planktonic bloom-forming cyanobacteria worldwide. 28,29 M. aeruginosa BLCC-F108 is a high-MC-producing strain that was isolated from Lake Okeechobee, Florida, during a bloom in 2019 and cultured at UF/IFAS. Prior to the experiment, a 4 mL cyanobacterial culture aliquot was sonicated for 5 min. Then, the 100 µL MC-LR (>95%, Cayman Chemical, Ann Arbor, MI) aqueous solution (500 μ g/mL) was spiked to the cyanobacterial solution. This MC-LR-spiked cyanobacterial solution was nebulized into the UF-APHOR chambers for the atmospheric aging of the MC-LR in cyanobacterial aerosols over the period of a day. Silica particles (NanoCym Inc.) were also employed to investigate the impact of aerosol media on the degradation of MC-LR. The 6 mg dry silica particles and the 100 μ L MC-LR aqueous solution (500 μ g/mL) were added to 5 mL of water and nebulized into the chamber.

The experimental conditions for each of the chamber runs are shown in Table 1 and Figure S3. A detailed description of the chamber, experimental procedures, and instrumentation can also be found in the Supporting Information. In brief, all chemicals and aerosols were injected early enough to allow for stabilization and measurement before reactions began at sunrise. The reaction of MC-LR in aerosol with ozone was performed at night to prevent the photochemical reactions. Ozone was produced using an ozone generator (Waterzone 500) and introduced into the chamber prior to cyanobacterial aerosol injection. Gas phase concentrations of NO_x and O_3 were measured using a Teledyne model 200E chemiluminescence NO-NO_x analyzer and a model 400E photometric O₃ analyzer, respectively. Particle distribution and number concentrations were measured with a scanning mobility particle sizer (SMPS) (TSI, model 3025A) coupled with a condensation nucleus counter (TSI, model 3022). Nonrefractory species (sulfate, nitrate, ammonium, chloride, and organics) in submicrometer aerosol were measured in situ by using an aerosol chemical speciation monitor (ACSM, Aerodyne). Both gas data (i.e., ozone) and aerosol data were corrected for chamber dilution using CCl₄ (>99.9%, Sigma-Aldrich) vaporized to the chamber.

Aerosol Collection. A particle-into-liquid sampler (PILS, Applikon, ADI 2081) was used to collect aerosols within a small amount of water at an air flow rate of 14.2 L/min. ^{30–33} The PILS samples collected in this were subsequently used for LC-MS/MS and the ELISA.

MC-LR Quantitation Using the ELISA and LC-MS/MS. Total MC-LR from the collected aerosol samples was determined within the background and treatments using an ADDA-microcystin/nodularin ELISA according to the manufacturer's protocols (Abraxis, Warminster, PA). Samples outside of the ELISA quantifiable range were diluted with doubly distilled water (18 Ω). The concentrations of MC-LR in the collected aerosol samples were also analyzed by high-performance liquid chromatography/tandem mass spectrometry (HPLC-MS/MS) using a model 6500 QTRAP instrument

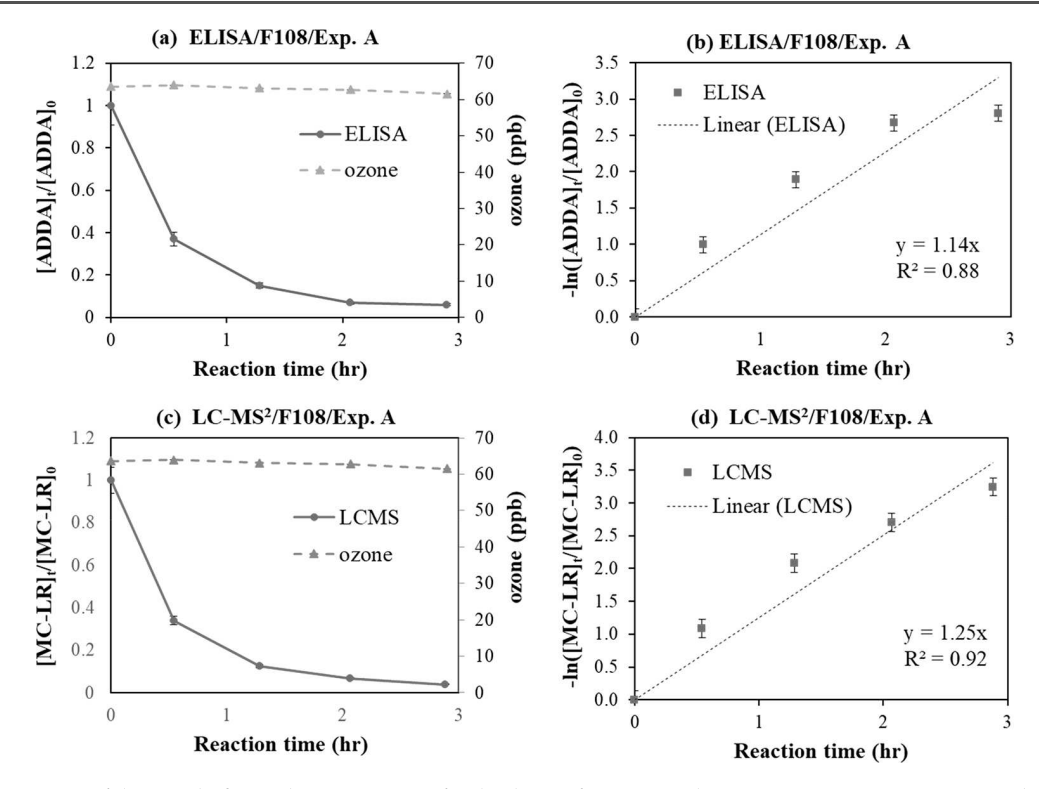


Figure 1. Determination of the pseudo-first-order rate constant for the decay of MC-LR in the *M. aeruginosa* BLCC-F108 cyanobacterial aerosol at a given ozone concentration (61.5 nm³ m⁻³). The ozone concentrations at night were almost constant (experiment A). Time profiles of (a) relative ADDA-based ELISA responses and (c) relative LC-MS/MS concentrations over the course of the chamber experiment. The measured rate constant is (b) $(3.91 \pm 0.17) \times 10^5 \text{ s}^{-1} \text{ L mol}^{-1}$ for the ADDA-based ELISA and (d) $(4.29 \pm 0.14) \times 10^5 \text{ s}^{-1} \text{ L mol}^{-1}$ for LC-MS/MS. The errors associated with the relative ELISA data and the relative LC-MS/MS data are estimated by using the propagation error with the individual errors in SMPS (estimation of the aerosol mass concentration), LC-MS/MS, and ELISA data.

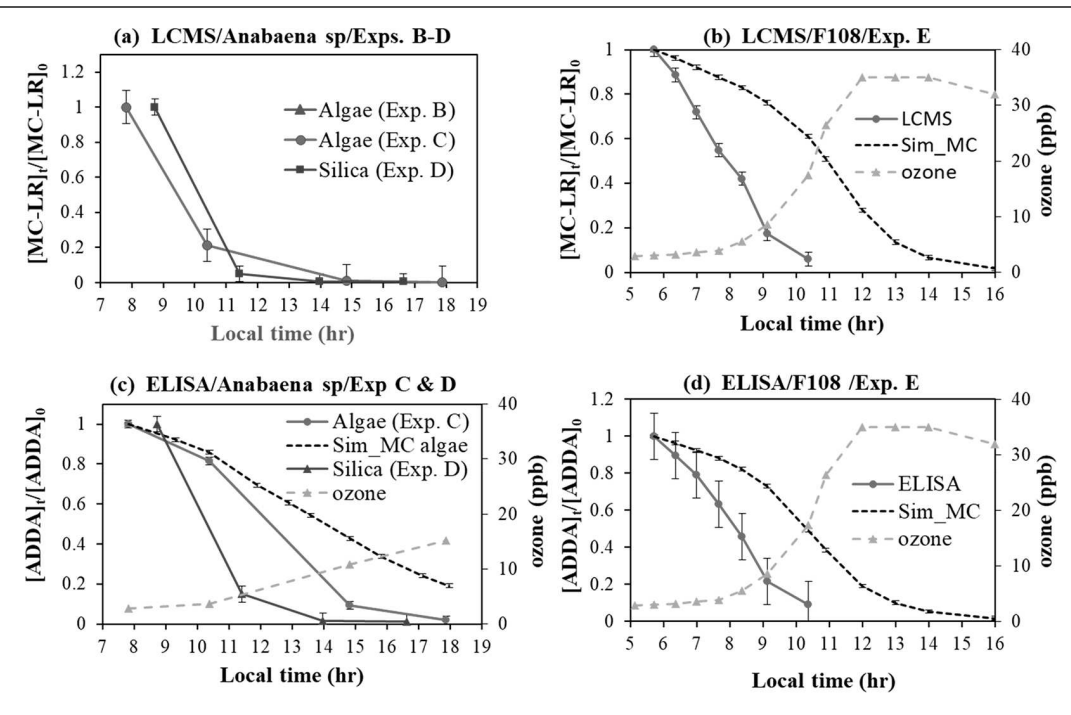


Figure 2. Time profiles of (a and b) relative MC-LR concentrations (LC-MS/MS) and (c and d) relative ADDA-based ELISA responses during the chamber experiment. "Sim-MC" in panel b indicates the prediction of the decay of aerosolized MC-LR by using $k_{\text{LCMS,ozone}}$ and ozone data from experiment E. For "Sim-MC" in panels c and d, $k_{\text{ADDA,ozone}}$ was integrated with ozone concentrations of experiments C and E, respectively, to predict the ADDA decay in aerosolized MC-LR during the day. The errors associated with relative concentrations are estimated by using the propagation error with the individual error in SMPS (estimation of the aerosol mass concentration), PILS, LC-MS/MS, and ELISA data.

(Sciex, Palo Alto, CA) coupled to a Nexera 2 UPLC (Shimadzu) system. Chromatographic separation was achieved on an Eclipse plus C18 column (2.1 mm × 100 mm, 3.5 mm) (Agilent, Santa Clara, CA). A detailed description of the LC-MS/MS operational conditions can be found in the Supporting Information.

■ RESULTS AND DISCUSSION

Relative Concentrations of MC-LR in Cyanobacterial Aerosols. The initial geometric mean diameter of the cyanobacterial particles in experiment A was 65 nm and grew to 135 nm (geometric standard deviation of 1.87-2.08) during the course of the experiment due to the coagulation of the particles. ACSM data showed that nitrogen-containing carbonaceous organic compounds could be mainly attributed to cyanobacterial aerosol compositions. Inorganic species, such as sulfate and chloride ions, were negligible. The nitrate in ACSM presumably originates from nitrogen-containing organic compounds in cyanobacterial aerosols. Both LC-MS/MS data (nanograms per milliliter) and ADDA based-ELISA data were normalized with the aerosol mass concentration (micrograms per milliliter). The aerosol mass concentration was obtained using SMPS data, the PILS sampling flow rate (14.2 L/min), the sampling duration (minutes), and the liquid mass collected using PILS. Then, the MC-LR concentration (nanograms per microgram) at time t ([MC-LR]_t) was normalized with the initial MC-LR concentration ([MC-LR]₀) at time zero. Figure 1 illustrates the time profiles of [MC-LR]_t/[MS-LR]₀ measured by LC-MS/MS, [ADDA]_t/[ADDA]₀ using ELISA data, and ozone concentrations at night. Figure 2 shows the daytime profiles of the ozone concentration and the relative MC-LR concentrations determined using LC-MS/MS and the

Difference in MC-LR Data between LC-MS/MS and the ELISA. Both LC-MS/MS and the ELISA suggest that MC-LR in cyanobacterial aerosols rapidly decays (Figures 1 and 2). Overall, MC-LR concentrations measured using LC-MS/MS showed more rapid decreases than those measured by the ELISA. The major epitope for the ELISA is the ADDA moiety,³⁴ and thus decreases in the ELISA focus on the degradation of ADDA in MC-LR. However, the decay of MC-LR measured by LC-MS/MS is attributed to the oxidation of the toxin in a variety of moieties, although the ADDA unit makes a larger contribution to the change in MC-LR.³⁵ In this study, we examined the important atmospheric pathways: (1) heterogeneous ozonolysis of MC-LR and (2) heterogeneous oxidation of MC-LR with atmospheric OH radicals.

Decay of MC-LR with Ozone. Ozone is produced during the photochemical cycle of NO_x integrated with the atmospheric oxidation of hydrocarbons. Ozone is frequently found, for example, in background air ranging from 20 to 60 nm³ m⁻³ near urban areas, as well as lakes and coastal areas. In terms of the MC-LR structure, the dien functionality of ADDA (Figure S1) can rapidly react with ozone. To avoid degradation of MC-LR via photochemical reactions, ozonolysis of MC-LR in the cyanobacterial aerosol was measured at night (experiment A, Figure 1). During the aging period, the ozone concentration was almost constant (decreasing from 63 to 61 nm³ m⁻³). Thus, the second-order rate constant ($k_{\rm ADDA,ozone}$) of ADDA with ozone was determined via a pseudo-first-order approach. For ELISA data, the degradation of ADDA in the cyanobacterial aerosol is expressed as

$$\frac{\text{d[ADDA]}}{\text{d}t} = -k_{\text{ADDA,ozone}}[\text{ozone}]_{\text{p}}[\text{ADDA}]$$
(1)

The ozone concentration ($[ozone]_p$) in the aerosol phase is estimated from the gaseous ozone concentration and the Henry's law constant (0.013 mol kg⁻¹ bar⁻¹ at 293 K).³⁷ The relative concentrations ([ADDA]_t/[ADDA]₀) were applied to determine the rate constant for the reaction of ADDA in cyanobacterial aerosol with ozone (Figure 1a,b). The estimated $k_{\rm ADDA,ozone}$ at 292 K is $(3.91 \pm 0.17) \times 10^5 \,\mathrm{M}^{-1} \,\mathrm{s}^{-1}$, showing the similar order for the ozone reaction of alkenes in the aqueous phase (Figure 1b).38 The reaction rate constant of MC-LR ($k_{LCMS,ozone}$) measured using LC-MS/MS data ([MC-LR]_t/[MC-LR]₀) is $(4.29 \pm 0.14) \times 10^5 \text{ M}^{-1} \text{ s}^{-1}$ (Figure 1c,d) showing a constant slightly larger than $k_{\mathrm{ADDA,ozone}}$ (statistically significant). The ELISA mainly detects the change in ADDA, but LC-MS/MS measures any chemical modification in MC-LR. Although the ozonolysis of the carbonyl-conjugated alkene of methyl-dehydroalanine (Mdha) in MC-LR (Figure S1) is much slower than the dien of ADDA, this alkene with an electron-withdrawing group can react with ozone (resulting in $k_{\text{LCMS,ozone}} > k_{\text{ADDA,ozone}}$). For example, the rate constant of isoprene (diene) is 12.8×10^{-18} cm³ molecule⁻¹ s⁻¹ at 298 K and that of acrolein (conjugated carbonyl) is 2.9×10^{-19} cm³ molecule⁻¹ s⁻¹.¹⁸

Decay of MC-LR in Sunlight. Similar to the trend in ozonolysis (Figure 1), MC-LR decay in LC-MS/MS was also faster than that in the ELISA, showing that amino acid units other than ADDA can be oxidized for the aging period (Figure 2a vs Figure 2c and Figure 2b vs Figure 2d). In the presence of cyanobacterial (*Anabaena*) aerosols (experiments B–D), the MC-LR decay in LC-MS/MS varied due to the difference in sunlight intensity: MC-LR decay in experiment B > MC-LR decay in experiment C. Experiment C was performed on a very cloudy day (high overcast), and sunlight irradiances were <10 W/m² for most aging periods (Figure S3). Furthermore, it was rainy or very cloudy the entire week the day before experiment C. Thus, there might have been little carryover of OH radicals from the previous day.

In the experiment on February 21, 2020, the decay of MC-LR in cyanobacterial aerosols (experiment C) was also compared to that in aerosolized silica particles (experiment D), which have no photoactivated pigment (Figure 2a,c). The surfaces of silica particles at high RHs (74-100% in Table 1) form a multilayer of water because they can contain a significant amount of water molecules at ambient RH (>20%) via a thermodynamic equilibrium process.^{39,40} Thus, MC-LR can dissolve in this water layer. Although the MC-LR decay in silica aerosol was faster than that in cyanobacterial aerosols, it is difficult to compare the MC-LR decay rates between the two experiments, because of the lack of data points associated with alternating sampling between two chambers using the single PILS. However, the rapid MC-LR decay in silica particles clearly evinces that aerosolized MC-LR is oxidized mainly via heterogeneous oxidation. We conclude that the effect of the photosensitizer in algal pigments (e.g., chlorophyll) on MC-LR degradation might be insignificant in air.

During the day, ozone can form in the outdoor chamber due to the photochemical reactions of hydrocarbons in the presence of a small amount of NO_x (2–10 nm³ m⁻³). A small amount of the gaseous photochemical initiators formaldehyde (6–18 nm³ m⁻³), acetaldehyde (2–6 nm³ m⁻³), and HONO also exists in chamber air. Additionally, semivolatile

hydrocarbons can be off gassing from the chamber wall to the chamber air. $k_{\text{ADDA,ozone}}$ and $k_{\text{LCMS,ozone}}$ were integrated with the ozone concentration in chamber air to predict the decay of aerosolized MC-LR during the day (Figure 2b-d).

Particularly for experiment E, the sampling of *M. aeruginosa* aerosols began before sunrise (local sunrise time, 6:45 a.m.) and continued through late morning. As one can see in panels b and d of Figure 2, the observed MC-LR decays measured with LC-MS/MS or the ELISA were much faster than the simulation using ozone profiles and ozonolysis rate constants ($k_{\rm ADDA,ozone}$ and $k_{\rm LCMS,ozone}$). This result suggests that different pathways other than ozonolysis contribute to aging of MC-LR. For example, the dien in ADDA can also react with the OH radicals that were carried forward from the previous day or formed through the photooxidation of hydrocarbons in the presence of NO_x .

We conclude that under ambient sunlight, MCs in aerosolized cyanobacteria heterogeneously decay via the reaction with ozone and possibly with OH radicals. At night, ozone presumably would be the dominant oxidant. The estimated lifetime of MC-LR is 111 min in the presence of 30 nm³ m⁻³ ozone (typical ambient ozone concentrations during the day) using $k_{\text{ADDA.ozone}}$. During the sunlight conditions of experiment E, the simulated lifetime of ADDA using the sole ozone process is almost 3 times longer than the observed lifetime, suggesting the possibility of the involvement of OH radicals. The rate of reaction of ADDA with OH radicals in the aerosol phase can be several times higher than that with ozone due to its high reactivity with dien (7 order of magnitude difference based on gas phase rate constants), although the quantity of OH radicals in aerosols is much smaller than that of ozone (estimation using typical gas phase concentrations and Henry's constants). Reducing 87.3% $(1/2^3)$ of ADDA in experiment E during the day takes 77 min. Assuming a gentle breeze (wind speed of 10 km/h), the residential areas within a 12.8 km distance of a cyanobacterial bloom source could be impacted by the harmful algal aerosols (at 87.5% ELISA decay with the conditions of experiment E). A stronger wind can dilute air plumes but travel longer distances.

For a more in-depth understanding, the decay rate constant $(k_{\rm ADDA,ozone})$ or $k_{\rm LCMS,ozone})$ of a variety of MC congeners with ozone needs to be explored in the future. The reaction of MCs with OH radicals needs to be further investigated. The individual rate constants of ADDA with each oxidant improve the simulation in its prediction of the impact of harmful algal aerosols on coastal and lake communities. The ROS can also be produced by the photosensitizing of pigments in cyanobacterial aerosols. ²² The significance of ROS with respect to the modulation of algal aerosol composition and the decay of toxins needs to be determined.

ASSOCIATED CONTENT

Supporting Information

The Supporting Information is available free of charge at https://pubs.acs.org/doi/10.1021/acs.estlett.0c00464.

Molecular structure of MC-LR (Figure S1), UF-APHOR chambers and instrumentation (Figure S2), detailed description of the chamber, experimental procedures, and instrumentation (section S1), and time profiles of temperature, relative humidity, and sunlight (irradiance) during the experiments using a large outdoor photochemical reactor (Figure S3) (PDF)

AUTHOR INFORMATION

Corresponding Author

Authors

- **David E. Berthold** Agronomy Department, Fort Lauderdale Research and Education Center, University of Florida, Davie, Florida 33314, United States
- Zechen Yu Department of Environmental Engineering Sciences, University of Florida, Gainesville, Florida 32611, United States; © orcid.org/0000-0002-6763-0520
- Cecilia Silva-Sanchez Department of Physiological Sciences and Center for Environmental and Human Toxicology, University of Florida, Gainesville, Florida 32608, United States
- H. Dail Laughinghouse IV Agronomy Department, Fort Lauderdale Research and Education Center, University of Florida, Davie, Florida 33314, United States
- Nancy D. Denslow Department of Physiological Sciences and Center for Environmental and Human Toxicology, University of Florida, Gainesville, Florida 32608, United States
- Sanghee Han Department of Environmental Engineering Sciences, University of Florida, Gainesville, Florida 32611, United States

Complete contact information is available at: https://pubs.acs.org/10.1021/acs.estlett.0c00464

Author Contributions

M.J. was responsible for chamber operation, data processing, data interpretation, and the preparation of the manuscript. Z.Y. and S.H. conducted chamber experiments with M.J. D.E.B. and H.D.L. were in charge of the ELISA and BLCC strain identification and culturing. C.S.-S. and N.D.D. were responsible for the determination of MC-LR concentration using LC-MS/MS.

Notes

The authors declare no competing financial interest.

ACKNOWLEDGMENTS

This research was supported by the National Science Foundation (1923651).

■ REFERENCES

- (1) Carmichael, W. W.; Boyer, G. L. Health impacts from cyanobacteria harmful algae blooms: Implications for the North American Great Lakes. *Harmful Algae* **2016**, *54*, 194–212.
- (2) Carmichael, W. W.; Falconer, I. R. Diseases related to freshwater blue-green algal toxins, and control measures; Academic Press: London, 1993.
- (3) Carmichael, W. W.; Azevedo, S. M.; An, J. S.; Molica, R. J.; Jochimsen, E. M.; Lau, S.; Rinehart, K. L.; Shaw, G. R.; Eaglesham, G. K. Human fatalities from cyanobacteria: chemical and biological evidence for cyanotoxins. *Environ. Health Perspect.* **2001**, *109*, 663–668.
- (4) Kirkpatrick, B.; Fleming, L. E.; Squicciarini, D.; Backer, L. C.; Clark, R.; Abraham, W.; Benson, J.; Cheng, Y. S.; Johnson, D.; Pierce, R.; Zaias, J.; Bossart, G. D.; Baden, D. G. Literature review of Florida red tide: implications for human health effects. *Harmful Algae* **2004**, *3*, 99–115.
- (5) Moore, S. K.; Trainer, V. L.; Mantua, N. J.; Parker, M. S.; Laws, E. A.; Backer, L. C.; Fleming, L. E. Impacts of climate variability and

- future climate change on harmful algal blooms and human health. Environ. Health 2008, 7, S4.
- (6) Grattan, L. M.; Holobaugh, S.; Morris, J. G. Harmful algal blooms and public health. *Harmful Algae* **2016**, *57*, 2–8.
- (7) Wells, M. L.; Trainer, V. L.; Smayda, T. J.; Karlson, B. S. O.; Trick, C. G.; Kudela, R. M.; Ishikawa, A.; Bernard, S.; Wulff, A.; Anderson, D. M.; Cochlan, W. P. Harmful algal blooms and climate change: Learning from the past and present to forecast the future. *Harmful Algae* 2015, 49, 68–93.
- (8) Mbukwa, E. A.; Msagati, T. A. M.; Mamba, B. B. Quantitative variations of intracellular microcystin-LR, -RR and -YR in samples collected from four locations in Hartbeespoort Dam in North West Province (South Africa) during the 2010/2011 summer season. *Int. J. Environ. Res. Public Health* **2012**, *9*, 3484–3505.
- (9) Duan, X.; Sanan, T.; de la Cruz, A.; He, X.; Kong, M.; Dionysiou, D. D. Susceptibility of the Algal Toxin Microcystin-LR to UV/Chlorine Process: Comparison with Chlorination. *Environ. Sci. Technol.* **2018**, 52, 8252–8262.
- (10) Heisler, J.; Glibert, P. M.; Burkholder, J. M.; Anderson, D. M.; Cochlan, W.; Dennison, W. C.; Dortch, Q.; Gobler, C. J.; Heil, C. A.; Humphries, E.; Lewitus, A.; Magnien, R.; Marshall, H. G.; Sellner, K.; Stockwell, D. A.; Stoecker, D. K.; Suddleson, M. Eutrophication and harmful algal blooms: A scientific consensus. *Harmful Algae* **2008**, *8*, 3–13.
- (11) May, N. W.; Olson, N. E.; Panas, M.; Axson, J. L.; Tirella, P. S.; Kirpes, R. M.; Craig, R. L.; Gunsch, M. J.; China, S.; Laskin, A.; Ault, A. P.; Pratt, K. A. Aerosol Emissions from Great Lakes Harmful Algal Blooms. *Environ. Sci. Technol.* **2018**, *52*, 397–405.
- (12) Wilson, A. E.; Sarnelle, O.; Neilan, B. A.; Salmon, T. P.; Gehringer, M. M.; Hay, M. E. Genetic Variation of the Bloom-Forming Cyanobacterium Microcystis aeruginosa within and among Lakes: Implications for Harmful Algal Blooms. *Appl. Environ. Microbiol.* **2005**, *71*, 6126.
- (13) Watanabe, M. F.; Oishi, S. Effects of Environmental Factors on Toxicity of a Cyanobacterium (Microcystis aeruginosa) under Culture Conditions. *Appl. Environ. Microbiol.* **1985**, *49*, 1342.
- (14) Olson, N. E.; Cooke, M. E.; Shi, J. H.; Birbeck, J. A.; Westrick, J. A.; Ault, A. P. Harmful Algal Bloom Toxins in Aerosol Generated from Inland Lake Water. *Environ. Sci. Technol.* **2020**, *54*, 4769–4780.
- (15) Young, F. M.; Metcalf, J. S.; Meriluoto, J. A. O.; Spoof, L.; Morrison, L. F.; Codd, G. A. Production of antibodies against microcystin-RR for the assessment of purified microcystins and cyanobacterial environmental samples. *Toxicon* **2006**, *48*, 295–306.
- (16) Mountfort, D. O.; Holland, P.; Sprosen, J. Method for detecting classes of microcystins by combination of protein phosphatase inhibition assay and ELISA: comparison with LC-MS. *Toxicon* **2005**, *45*, 199–206.
- (17) Samdal, I. A.; Ballot, A.; Løvberg, K. E.; Miles, C. O. Multihapten Approach Leading to a Sensitive ELISA with Broad Cross-Reactivity to Microcystins and Nodularin. *Environ. Sci. Technol.* **2014**, *48*, 8035–8043.
- (18) Finlayson-Pitts, B. J.; Pitts, J. N. Chemistry of the upper and lower atmosphere: Theory, Experiments, and Applications; Academic Press: New York, 2000.
- (19) Hallquist, M.; Wenger, J. C.; Baltensperger, U.; Rudich, Y.; Simpson, D.; Claeys, M.; Dommen, J.; Donahue, N. M.; George, C.; Goldstein, A. H.; Hamilton, J. F.; Herrmann, H.; Hoffmann, T.; Iinuma, Y.; Jang, M.; Jenkin, M. E.; Jimenez, J. L.; Kiendler-Scharr, A.; Maenhaut, W.; McFiggans, G.; Mentel, T. F.; Monod, A.; Prévôt, A. S. H.; Seinfeld, J. H.; Surratt, J. D.; Szmigielski, R.; Wildt, J. The formation, properties and impact of secondary organic aerosol: current and emerging issues. *Atmos. Chem. Phys.* **2009**, *9*, 5155–5236.
- (20) Schaefer, A. M.; Yrastorza, L.; Stockley, N.; Harvey, K.; Harris, N.; Grady, R.; Sullivan, J.; McFarland, M.; Reif, J. S. Exposure to microcystin among coastal residents during a cyanobacteria bloom in Florida. *Harmful Algae* **2020**, *92*, 101769.
- (21) Ledford, H. K.; Niyogi, K. K. Singlet oxygen and photo-oxidative stress management in plants and algae. *Plant, Cell Environ.* **2005**, 28, 1037–1045.

- (22) Triantaphylidès, C.; Havaux, M. Singlet oxygen in plants: production, detoxification and signaling. *Trends Plant Sci.* **2009**, *14*, 219–228.
- (23) Firmer, A. A. Singlet Oxygen Vol. 1: Physical-Chemical Aspects; CRC Press: Cleveland, 1985.
- (24) Jang, M.; McDow, S. R. Benz[a]anthracene photodegradation in the presence of known organic constituents of atmospheric aerosols. *Environ. Sci. Technol.* **1995**, *29*, 2654–2660.
- (25) Im, Y.; Jang, M.; Beardsley, R. Simulation of Aromatic SOA Formation Using the Lumping Model Integrated with Explicit Gas-Phase Kinetic Mechanisms and Aerosol Phase Reactions. *Atmos. Chem. Phys. Discuss.* **2013**, *13*, 5843–5870.
- (26) Beardsley, L. R.; Jang, M. Simulating the SOA formation of isoprene from partitioning and aerosol phase reactions in the presence of inorganics. *Atmos. Chem. Phys.* **2016**, *16*, 5993–6009.
- (27) Zhou, C.; Jang, M.; Yu, Z. Simulation of SOA Formation from the Photooxidation of Monoalkylbenzenes in the Presence of Aqueous Aerosols Containing Electrolytes under Various NO_x Levels. *Atmos. Chem. Phys.* **2019**, *19*, 5719–5735.
- (28) Laughinghouse, H. D.; Prá, D.; Silva-Stenico, M. E.; Rieger, A.; Frescura, V. D.-S.; Fiore, M. F.; Tedesco, S. B. Biomonitoring genotoxicity and cytotoxicity of Microcystis aeruginosa (Chroococales, Cyanobacteria) using the Allium cepa test. *Sci. Total Environ.* **2012**, 432, 180–188.
- (29) Werner, V. R.; Laughinghouse, H. D., IV Bloom-forming and other planktonic Anabaena (Cyanobacteria) morphospecies with twisted trichomes from Rio Grande do Sul State, Brazil. *Nova Hedwigia* **2009**, *89*, 17–47.
- (30) Orsini, D. A.; Ma, Y.; Sullivan, A.; Sierau, B.; Baumann, K.; Weber, R. J. Refinements to the particle-into-liquid sampler (PILS) for ground and airborne measurements of water soluble aerosol composition. *Atmos. Environ.* **2003**, *37*, 1243–1259.
- (31) Jiang, H.; Jang, M. Dynamic Oxidative Potential of Atmospheric Organic Aerosol Under Ambient Sunlight. *Environ. Sci. Technol.* **2018**, 52, 7496–7504.
- (32) Jiang, H.; Jang, M.; Sabo-Attwood, T.; Robinson, S. E. Oxidative Potential of Secondary Organic Aerosols Produced from Photooxidation of Different Hydrocarbons Using Outdoor Chamber under Ambient Sunlight. *Atmos. Environ.* **2016**, *131*, 382–389.
- (33) Jiang, H.; Yu, Z.; Jang, M. Dithiothreitol Activity by Particulate Oxidizers of SOA Produced from Photooxidation of Hydrocarbons under Varied NO_x Levels. *Atmos. Chem. Phys.* **2017**, *17*, 9965–9977.
- (34) Fischer, W. J.; Garthwaite, I.; Miles, C. O.; Ross, K. M.; Aggen, J. B.; Chamberlin, A. R.; Towers, N. R.; Dietrich, D. R. Congener-Independent Immunoassay for Microcystins and Nodularins. *Environ. Sci. Technol.* **2001**, *35*, 4849–4856.
- (35) Campos, A.; Vasconcelos, V. Molecular Mechanisms of Microcystin Toxicity in Animal Cells. *Int. J. Mol. Sci.* **2010**, *11*, 268–287.
- (36) Dueñas, C.; Fernández, M. C.; Cañete, S.; Carretero, J.; Liger, E. Assessment of ozone variations and meteorological effects in an urban area in the Mediterranean Coast. *Sci. Total Environ.* **2002**, 299, 97–113.
- (37) Kosak-Channing, L. F.; Helz, G. R. Solubility of ozone in aqueous solutions of 0–0.6 M ionic strength at 5–30.degree.C. *Environ. Sci. Technol.* **1983**, *17*, 145–149.
- (38) Dowideit, P.; von Sonntag, C. Reaction of Ozone with Ethene and Its Methyl- and Chlorine-Substituted Derivatives in Aqueous Solution. *Environ. Sci. Technol.* **1998**, *32*, 1112–1119.
- (39) Yu, Z.; Jang, M. Simulation of Heterogeneous Photooxidation of SO₂ and NO_x in the Presence of Gobi Desert Dust Particles Unver Ambient Sunlight. *Atmos. Chem. Phys.* **2018**, *18*, 14609–14622.
- (40) Park, J.; Jang, M.; Yu, Z. Heterogeneous Photooxidation of SO₂ in the Presence of Two Different Mineral Dust Particles: Gobi and Arizona Dust. *Environ. Sci. Technol.* **2017**, *51*, 9605–9613.